Earth and Planetary Science Letters 384 (2013) 37–41

Contents lists available at ScienceDirect

Earth and Planetary Science Letters

www.elsevier.com/locate/epsl

Detectability of thermal signatures associated with active formation of 'chaos terrain' on Europa

Oleg Abramov [a,*], Julie A. Rathbun [b], Britney E. Schmidt [c], John R. Spencer [d]

[a] U.S. Geological Survey, Astrogeology Science Center, 2255 N. Gemini Dr., Flagstaff, AZ 86001, USA
[b] Planetary Science Institute, 1700 E. Fort Lowell Rd., Suite 106, Tucson, AZ 85719-2395, USA
[c] Georgia Institute of Technology, School of Earth and Atmospheric Sciences, 311 Ferst Dr., Atlanta, GA 30312, USA
[d] Southwest Research Institute, 1050 Walnut St., Suite 300, Boulder, CO 80302, USA

ARTICLE INFO

Article history:
Received 21 February 2013
Received in revised form 12 September 2013
Accepted 20 September 2013
Available online 26 October 2013
Editor: C. Sotin

Keywords:
Europa
chaos
endogenic heat
thermal modeling
thermal mapping
spacecraft instruments

ABSTRACT

A recent study by Schmidt et al. (2011) suggests that Thera Macula, one of the "chaos regions" on Europa, may be actively forming over a large liquid water lens. Such a process could conceivably produce a thermal anomaly detectable by a future Europa orbiter or flyby mission, allowing for a direct verification of this finding. Here, we present a set of models that quantitatively assess the surface and subsurface temperatures associated with an actively resurfacing chaos region using constraints from Thera Macula. The results of this numerical study suggest that the surface temperature over an active chaos region can be as high as ~200 K. However, low-resolution Galileo Photo-Polarimeter Radiometer (PPR) observations indicate temperatures below 120 K over Thera Macula. This suggests that Thera Macula is not currently active unless an insulating layer of at least a few centimeters in thickness is present, or activity is confined to small regions, reducing the overall intensity of the thermal signature. Alternatively, Thera may have been cooling for at least 10–100 yr and still contain a subsurface lake, which can take ~300,000 yr to crystallize. According to the present study, a more sensitive instrument capable of detecting anomalies ~ 5 K above ambient could detect activity at Thera Macula even if an insulating layer of ~50 cm is present.

Published by Elsevier B.V.

1. Introduction and objectives

Jupiter's innermost icy Galilean satellite Europa appears to possess a ~100 km deep briny ocean beneath its few-to-tens-of-km-thick outer ice shell (e.g., Greenberg et al., 2000; Billings and Kattenhorn, 2005), as suggested by surface morphology (e.g., Carr and et al., 1998; Hoppa et al., 1999; Pappalardo et al., 1999), and Galileo magnetometer measurements (e.g., Khurana et al., 1998; Kivelson et al., 2000). A wide variety of resurfacing features have been observed, including small (< ~10 km), dark subcircular bumps or depressions (lenticulae), bands, ridges, regions of disrupted crust termed 'chaos terrains', and possible cryovolcanic features, which consist of apparent flooding of portions of Europa's surface (e.g., Pappalardo et al., 1999). This suggests a strong possibility of ongoing endogenic activity, probably driven by tidal effects caused by the Laplace resonance of Europa with Io and Ganymede (e.g., Cassen et al., 1979, 1980; Greenberg et al., 1998; Hussmann and Spohn, 2004), which is supported by a young average surface age of ~40–90 Ma (Zahnle et al., 1998; Pappalardo et al., 1999; Schenk et al., 2004; Bierhaus et al., 2009).

Many of these resurfacing events likely deliver warm material from depth to the near-surface and thus produce an associated thermal anomaly. Although the Galileo Photo-Polarimeter Radiometer (PPR) instrument did not detect any endogenic anomalies, that may be due to its low resolution (see "Constraints from Galileo PPR" section), and they may be detectable by a more sophisticated thermal mapping instrument on a future Europa mission. Abramov and Spencer (2008) modeled such anomalies as bodies of warm ice or liquid water emplaced onto the surface, predicting diurnal surface temperature variations over the thermal anomaly, as well as detectable lifetimes, which ranged from tens to thousands of years, depending on the initial thickness of the water or ice layer. The study also predicted that the number of detectable thermal anomalies on Europa should be on the order of 1 to 10, if recent resurfacing is dominated by chaos regions and resurfacing events occur at regular intervals.

Perhaps the biggest weakness of the Abramov and Spencer (2008) work was that, at the time, there was a dearth of observational or theoretical constraints regarding the size or depth of possible present-day water layers in the ice shell. This has recently changed with the publication of Schmidt et al. (2011), who analyzed topography and geomorphology of Conamara Chaos

* Corresponding author.
E-mail addresses: oabramov@usgs.gov (O. Abramov), julie_rathbun@redlands.edu (J.A. Rathbun), britneys@ig.utexas.edu (B.E. Schmidt), spencer@boulder.swri.edu (J.R. Spencer).

0012-821X/$ – see front matter Published by Elsevier B.V.
http://dx.doi.org/10.1016/j.epsl.2013.09.027

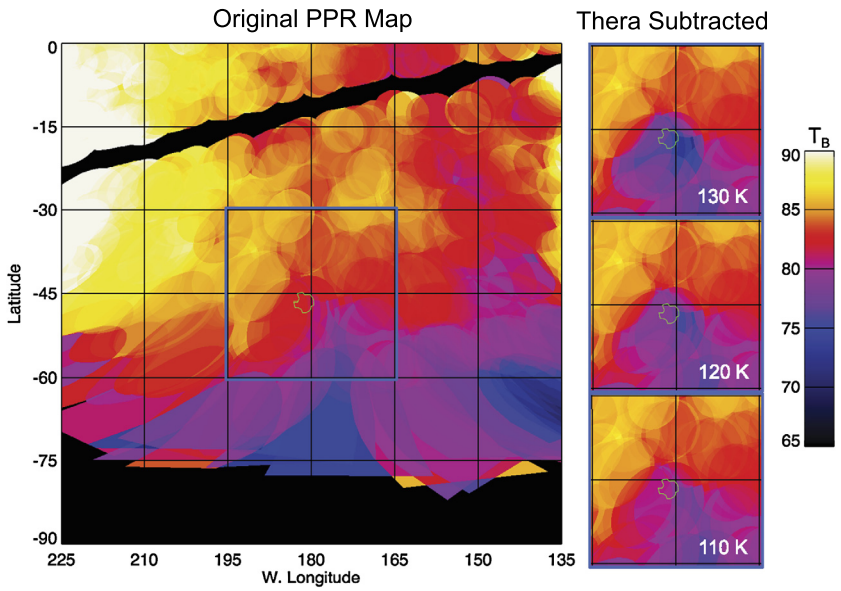

Fig. 1. Left: A nighttime brightness temperature map of part of Europa's surface centered on Thera Macula (green outline), derived from the Galileo PPR observation 25EPDRKMAP01 taken in November 25th, 1999. Subsolar longitude was 40°W. The map was created by averaging the radiance observed from overlapping PPR fields of view, and the black region results from missing data. The blue box shows the region covered by the smaller maps on the right. Right: Part of the same temperature map after subtracting the flux expected from Thera Macula, assuming its nighttime temperature is 110, 120, or 130 K. An assumed Thera temperature greater than about 120 K requires implausibly low background temperatures for the surrounding region to match the observed fluxes. (For interpretation of the references to color in this figure legend, the reader is referred to the web version of this article.)

and Thera Macula Chaos regions, and developed a conceptual model that suggested the possible presence of a water lens ~3 km underneath Thera Macula that was liquid at the time of the Galileo encounter. These new developments provide an opportunity to apply the existing thermal model to a potential actively forming chaos region on Europa, with established constraints and estimates of latitude, ice and water thickness, and initial temperatures, to calculate what the thermal signature might be at the surface. The overall goal is to assess whether the thermal anomaly associated with Thera Macula, if one exists, is consistent with past data and whether it could be detected (and therefore confirmed) by a future Europa orbiter or flyby mission such as JUICE, which plans to conduct two flybys of Europa, one of them over Thera Macula (Grasset et al., 2013). In particular, we estimate surface temperature over an actively forming chaos region, taking sublimation cooling into account, as well as estimate the amount of time a surface thermal anomaly remains detectable after the active phase of formation ceases.

2. Constraints from Galileo PPR

The Galileo Photo-Polarimeter Radiometer (PPR) mapped the Thera region several times during Galileo's Europa flybys, but found no signs of endogenic activity (Spencer et al., 1999; Rathbun et al., 2010). Rathbun et al. (2010) determined the detection limits in the highest quality PPR datasets by adding synthetic unresolved thermal anomalies of various brightnesses to the data and noting the brightness at which these became detectable above the background, and created separate maps for data taken in each of 3 separate filters: 17 μm, 27 μm, and an open filter. The strongest temperature constraints come from the 25EPDRKMAP01 observation, obtained on Galileo's 25th orbit of Jupiter on November 25th, 1999 UT, through PPR's open filter. PPR scanned the Thera region at night at a local Europa time of 2:40 am and an emission angle of 50°. The projected diameter of PPR's circular field of view was 220 km × 340 km. It should be noted that actual surface kinetic temperatures are slightly higher than the infrared brightness temperatures measured by PPR, because emissivity is less than unity (Spencer et al., 1999). No flux enhancement was seen at Thera's location in the PPR data (Fig. 1, left). The region near Thera Macula was mapped with a detection limit of 2×10^3 W str^{-1} in the open filter (Rathbun et al., 2010), which, when adjusted for a nighttime background temperature of 82 K and the calculated 4180 km^2 area of Thera, yields a surface temperature of 113 K necessary to output the above power. The uncertainty in the detection limit is a factor of 2, which corresponds to an uncertainty in the temperature of approximately 10 K. Therefore, if Thera Macula had a surface temperature above 113 K, or 31 K above the observed background surface temperature, across the entire feature, the PPR instrument should have detected it. However, if only discrete regions within Thera Macula are experiencing ongoing resurfacing, these regions could be warmer and, with less aerial extent, go undetected.

In addition, we also employ a qualitative method of estimating the maximum plausible temperature for Thera Macula. For a range of assumed surface temperatures, we calculate Thera's flux contribution to each PPR field of view, accounting for the fractional filling factor of Thera's 4180 km^2 surface area in the field of view (never more than 6%) and subtract that flux from the observed flux. We then produce a Thera-subtracted surface temperature map of Europa (assuming blackbody radiation) for each assumed Thera temperature by averaging the flux from overlapping fields of view. Subtracting the flux from Thera temperatures of 120 K or greater produces a cold spot at Thera's location that is of a higher amplitude than cold spots seen elsewhere in the map (Fig. 1, right), so we derive an upper limit of about 120 K for the nighttime temperature of Thera from this PPR observation, which is consistent with the earlier calculation of 113 ± 10 K.

3. Numerical modeling

We employ a numerical thermal modeling code (available from authors) to track the surface and subsurface thermal evolution of Thera Macula. The vertical extent of the region of interest is only a few kilometers, whereas the horizontal dimension of Thera is ~70 km, allowing the application of a one-dimensional model to this problem. The code makes use of a commonly used explicit

Table 1
Summary of model runs. Layers are listed from top to bottom.

Run 1 – Baseline	Run 4 – 2-km water depth
3-km 235 K ice layer	3-km 235 K ice layer
3-km 273.15 K water layer	2-km 273.15 K water layer
4-km 235 K ice layer	5-km 235 K ice layer
Run 2 – Warm upper ice	Run 5 – 4-km water depth
3-km 272 K ice layer	3-km 235 K ice layer
3-km 273.15 K water layer	4-km 273.15 K water layer
4-km 235 K ice layer	3-km 235 K ice layer
Run 3 – Low water temp	
3-km 235 K ice layer	
3-km 250 K water layer (latent heat of freezing adjusted accordingly)	
4-km 235 K ice layer	

finite-difference method (e.g., Ketkar, 1999) to calculate transient heat conduction. The model also includes convection in liquid water, latent heat of fusion, depth- and temperature-dependent heat capacity and thermal conductivity, and, at the surface boundary, radiative cooling, rotational modulation of insolation, absorption of sunlight, and cooling by sublimation of surface ice (Eq. (1)). Convection within the ice is not included, as ice shells <5 km are stable to convective overturn (McKinnon, 1999).

The model consists of 1000 standard horizontal slabs and two boundary slabs at the top and bottom surfaces. Model temperatures are measured at nodes in the center of each slab. The resolution is 10 m per slab, with the exception of the uppermost slab, which is 5 m, placing the central node at the surface. The temporal resolution of the model is 1500 s per timestep, which satisfies conductive stability criteria at this spatial resolution. The modeled material is assumed to be pure liquid water or ice Ih, depending on the temperature, which is consistent with the phase diagram of water under the conditions in Europa's crust. The heat capacity and thermal conductivity of ice in the model vary as a function of temperature, as described by Murphy and Koop (2005) and Slack (1980), respectively. The temperature of the upper boundary of the model represents a balance between conductive heat flux from below, thermal radiation to space, absorbed sunlight, and sublimation cooling, which is described by the equation

$$\kappa\left(\frac{\partial T(z,t)}{\partial z}\right)_{z=0} = \varepsilon\sigma T^4(0,t) - (1-A)F_S(t) + Lp_v\sqrt{\frac{m}{2\pi RT}} \quad (1)$$

where κ is thermal conductivity, ε is emissivity, σ is the Stefan–Boltzmann constant, A is the bolometric albedo, L is the latent heat of sublimation, p_v is the vapor pressure of ice, m is the molecular weight of H_2O, R is the universal gas constant, and F_S is the time-dependent flux of incident sunlight, which cycles as Europa completes a rotation every 3.5512 Earth days. Bolometric albedo and emissivity are set to typical Europa values of 0.55 and 0.9, respectively (Spencer et al., 1999).

The baseline simulation (Run 1) models Thera Macula as a 3-km layer of 235 K ice, underlain by a 3-km layer of water at the freezing point of 273.15 K, which is in turn underlain by a 4-km layer of ice at 235 K. The bottom boundary is set to a constant "deep temperature" of 97.70 K, calculated by running the model with insolation as the only heat source. The lower ice layer represents the diminishing plume at ~235 K (Pappalardo et al., 1998), and the upper ice layer represents ice blocks surrounded by a water/ice matrix (Schmidt et al., 2011) with a mean temperature conservatively set to the same as the underlying plume. However, given the number of unknowns in the model, additional runs were set up to fully explore the possible parameter space (Table 1). One such parameter is the temperature of the uppermost ice layer, which

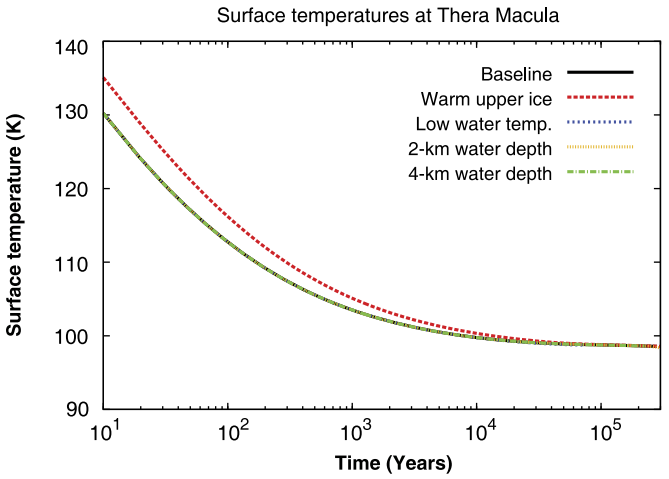

Fig. 2. Surface temperatures above the Thera Macula hotspot following the cessation of the plume and the end of active chaos formation. With the exception of Run 2 ("Warm upper ice"), surface temperature evolution is essentially identical for all parameters examined. Temperatures at timescales less than $\sim 10^1$ yr after end of active chaos formation are not reported due to the relatively coarse spatial resolution of the model.

modeling suggests can exceed 260 K (e.g., Showman and Han, 2005), and is modeled here at the maximum plausible temperature of 272 K (Run 2). Also, the pressure of the buoyant force of the plume against the ice overburden (Pappalardo and Barr, 2004), as well as the presence of impurities (Head and Pappalardo, 1999; Schmidt et al., 2011) can depress the freezing point of the liquid water lens, and we modeled a water layer with a low temperature of 250 K (Run 3). Finally, the work of Schmidt et al. (2011) estimated the thickness of the water lens at 2–4 km, and we include models with water depths of 2 km (Run 4) and 4 km (Run 5).

4. Modeling results

For all simulations the modeled surface temperature drops almost immediately to ~200 K due to a rapid heat loss by sublimation. This would be the equilibrium temperature if the plume remains active, and heat continues to be supplied to the surface. However, if plume activity ceases, active chaos formation will stop and surface temperatures will begin to decline. Fig. 2 shows the evolution of surface temperatures following plume cessation, and the result is essentially identical for all runs except for Run 2, which had a 272 K upper ice layer. This indicates that surface temperatures are controlled primarily by conditions in the near-surface, and the initial depth and temperature of the water, as well as the initial temperature of the underlying plume, have little to no effect.

The length of time that a thermal anomaly associated with a cooling Thera Macula-like chaos region remains detectable depends on the sensitivity of the infrared instrument and the characteristics of the surface. Although temperature differences as small as 1 K are in principle detectable from a Europa orbiter or flyby spacecraft, identification of an endogenic anomaly requires correction for albedo and thermal inertia effects, which may be difficult to do with a precision better than 5 K (Abramov and Spencer, 2008). The preliminary specifications for the Sub-millimeter Wave Instrument (SWI) on the planned Jupiter Icy Moon Explorer (JUICE) mission will allow it to perform thermal observations with an absolute accuracy of 2 K or better, and spatial resolution better than 30 km/pixel (JUICE Science Requirement Matrix draft, May 2012), which is significantly smaller than the ~70 km average diameter of Thera Macula. We therefore present results for detection criteria ranging from 1 K to 5 K above ambient (Table 2), which range

Table 2
Length of time that the surface thermal anomaly associated with Thera Macula remains detectable after the cessation of plume activity. Detection criteria are given in degrees above mean ambient surface temperature. Pure consolidated water ice is assumed.

Detection criteria	Detectable lifetime
Run 1 – Baseline	
5 K above ambient (102.81 K)	1330 Earth years
4 K above ambient (101.81 K)	2170 Earth years
3 K above ambient (100.81 K)	3990 Earth years
2 K above ambient (99.81 K)	9400 Earth years
1 K above ambient (98.81 K)	71,600 Earth years
Run 2 – Warm upper ice	
5 K above ambient (102.81 K)	2320 Earth years
4 K above ambient (101.81 K)	3760 Earth years
3 K above ambient (100.81 K)	6940 Earth years
2 K above ambient (99.81 K)	16,200 Earth years
1 K above ambient (98.81 K)	94,500 Earth years

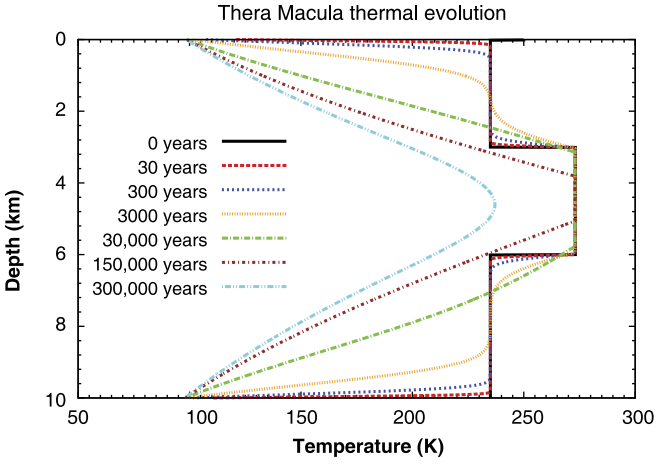

Fig. 3. Temperature profiles for Run 1 ("Baseline"), showing the subsurface thermal evolution of Thera Macula following the cessation of the plume and the end of active chaos formation.

from $\sim 10^3$ to $\sim 10^5$ yr. This implies that if Thera Macula was actively resurfacing at the time of the Galileo encounter, as suggested by Schmidt et al. (2011), the associated thermal anomaly should still remain detectable for the next $\sim 10^3$ yr, even if the plume has diminished or ceased.

The possible subsurface evolution of Thera Macula (Fig. 3) is also of interest, because a large body of liquid water underneath a thin ice crust would be a prime landing site for future missions. Our baseline model predicts that the time for a 3-km liquid water lens underneath Thera Macula to freeze completely is 2.85×10^5 yr, which is consistent with an estimate by Schmidt et al. (2011) of 10^5–10^6 yr. This duration is influenced by the initial temperature of the water and its assumed initial thickness, and ranges from 2.15×10^5 yr for a 2-km water layer to 3.43×10^5 yr for a 4-km water layer. A presence of a 15-m insulating surface layer (see below) extends the lifetime to 3.54×10^5 yr.

Simulations discussed so far assumed pure, consolidated, crystalline water ice. However, Voyager and Galileo observations of Europa (e.g., Spencer et al., 1999) found that the thermal inertia of the surface is $\sim 7 \times 10^4$ erg cm^{-2} s^{-1} K$^{-1/2}$, or $\sim$30 times lower than that of solid water ice (Hansen, 1972), implying a highly unconsolidated surface. The thermal inertia of the Thera Macula region is likewise $\sim 7 \times 10^4$ erg cm^{-2} s^{-1} K$^{-1/2}$ (Rathbun et al., 2010). The fact that the thermal inertia of Thera Macula is unremarkable compared to the surrounding areas might appear to be a circumstantial argument against active resurfacing in that region. It should be noted, however, that the processes responsible for low thermal inertias, and their timescale, are largely unknown (e.g., Rathbun et al., 2010). In addition, an unconsolidated surface can also be formed by the turbulent disruption of the ice/water matrix during freezing as a result of nucleation and growth of vapor bubbles (e.g. Cassen et al., 1979). In fact, the model of Schmidt et al. (2011) does not predict surface flows or ponded material, rather unconsolidated ice cracked and modified by the refreezing of the lens, and entrained water would be expected, as seen in ice mélange associated with calving fronts and collapsed ice shelves (e.g., Amundson et al., 2010; Scambos et al., 2009).

Table 3
Surface temperatures associated with an insulating layer (TI $= 7.0 \times 10^4$ erg-cgs) overlying warm ice at a constant temperature of 235 K. Note that although the absolute temperatures are significantly different between dawn and afternoon for each insulating layer thickness, ΔT due to endogenic heating is essentially the same.

Insulating layer thickness	Time of day	Surface temperature (K)	Degrees above ambient (K)
15 m	dawn	90.70	0.13
15 m	afternoon	104.68	0.12
1 m	dawn	92.99	2.42
1 m	afternoon	106.97	2.41
27.5 cm	dawn	98.16	7.59
27.5 cm	afternoon	112.12	7.56
7.5 cm	dawn	108.19	17.62
7.5 cm	afternoon	122.04	17.48

To evaluate the effects of the near-surface insulating layer with a thermal inertia of 7×10^4 erg cm^{-2} s^{-1} K$^{-1/2}$, several additional simulations were conducted. An end-member scenario was assumed, in which the lower thermal inertia is due solely to lower thermal conductivity. The results (Table 3) indicate that an insulating layer of 7.5 cm would have been sufficient to mask the thermal signature of 235 K ice to Galileo PPR, which required $\sim$30–40 K above background for detection. A more sensitive, higher-resolution thermal mapping instrument, however, could permit detection even if over 1 m of insulating material is present.

5. Conclusions

Galileo PPR detected no signs of endogenic activity at Thera Macula with a detection threshold of $\sim$30–40 K above background. Results of the numerical study suggest that the equilibrium surface temperature above an actively forming Thera Macula-like chaos region would be $\sim$200 K, and, once active formation ceases, the associated hotspot would remain detectable from visiting spacecraft for at least $\sim 10^3$ yr, possibly for as long as 10^5 yr, depending on the capabilities of the instrument, and if consolidated ice is assumed. The results further indicate that the time for a 3-km liquid water lens underneath Thera Macula to freeze completely is 2.85×10^5 yr, which is consistent with the Schmidt et al. (2011) estimate. The presence of a near-surface insulating layer, as well as reduced aerial exposure of the warm material, can decrease the thermal signature. For Galileo PPR, an insulating layer of only a few centimeters would have been sufficient to render the thermal anomaly undetectable. According to the present study, a more sensitive instrument could detect activity at Thera Macula even in the presence of an insulating layer of several meters, for a $\sim$1 K detection limit, or $\sim$50 cm, for a $\sim$5 K detection limit.

Acknowledgements

The authors thank Catherine Neish and an anonymous reviewer for fair, thorough, and constructive reviews of this manuscript. O.A. gratefully acknowledges support from the NASA Cassini Data Analysis Program under IAT # NNH13AV61I.

References

Abramov, O., Spencer, J.R., 2008. Numerical modeling of endogenic thermal anomalies on Europa. Icarus 195, 378–385.

Amundson, J.M., Fahnestock, M., Truffer, M., Brown, J., Lüthi, M.P., Motyka, R.J., 2010. Ice mélange dynamics and implications for terminus stability, Jakobshavn Isbræ, Greenland. J. Geophys. Res. 115, http://dx.doi.org/10.1029/2009JF001405.

Bierhaus, E.B., Zahnle, K., Chapman, C.R., 2009. Europa's crater distributions and surface ages. In: Pappalardo, R.T., McKinnon, W.B., Khurana, K.K. (Eds.), Europa. University of Arizona Press, Tucson, pp. 161–180.

Billings, S.E., Kattenhorn, S.A., 2005. The great thickness debate: Ice shell thickness models for Europa and comparisons with estimates based on flexure at ridges. Icarus 177, 397–412.

Carr, M.H., et al., 1998. Evidence for a subsurface ocean on Europa. Nature 391, 363–365.

Cassen, P.M., Reynolds, R.T., Peale, S.J., 1979. Is there liquid water on Europa?. Geophys. Res. Lett. 6, 731–734.

Cassen, P., Peale, S.J., Reynolds, R.T., 1980. Tidal dissipation in Europa: a correction. Geophys. Res. Lett. 7, 987–988.

Grasset, O., Dougherty, M.K., Coustenis, A., Bunce, E.J., Erd, C., Titov, D., Blanc, M., Coates, A., Drossart, P., Fletcher, L.N., Hussmann, H., Jaumann, R., Krupp, N., Lebreton, J.-P., Prieto-Ballesteros, O., Tortora, P., Tosi, F., Van Hoolst, T., 2013. JUpiter ICy moons Explorer (JUICE): An ESA mission to orbit Ganymede, to characterise the Jupiter system. Planet. Space Sci. 78, 1–21.

Greenberg, R., Geissler, P., Hoppa, G., Tufts, B.R., Durda, D.D., Pappalardo, R., Head, J.W., Greeley, R., Sullivan, R., Carr, M.H., 1998. Tectonic processes on Europa: tidal stresses, mechanical response, and visible features. Icarus 135, 64–78.

Greenberg, R., Geissler, P., Tufts, B.R., Hoppa, G.V., 2000. Habitability of Europa's crust: The role of tidal-tectonic processes. J. Geophys. Res. 105, 17551–17562.

Hansen, O.L., 1972. Thermal radiation from the Galilean satellites measured at 10 and 20 microns. PhD thesis, California Institute of Technology, Pasadena.

Head, J.W., Pappalardo, R.T., 1999. Brine mobilization during lithospheric heating on Europa: implications for formation of chaos terrain, lenticular texture, and color variations. J. Geophys. Res. 104, 27143–27155.

Hoppa, G.V., Tufts, B.R., Greenberg, R., Geissler, P.E., 1999. Formation of cycloidal features on Europa. Science 285, 1899–1902.

Hussmann, H., Spohn, T., 2004. Thermal–orbital evolution of Europa. Icarus 171, 391–410.

Ketkar, S.P., 1999. Numerical Thermal Analysis. American Society of Mechanical Engineers, New York.

Khurana, K.K., Kivelson, M.G., Stevenson, D.J., Schubert, G., Russell, C.T., Walker, R.J., Joy, S., Polanskey, C., 1998. Induced magnetic fields as evidence for subsurface oceans in Europa and Callisto. Nature 395, 777–780.

Kivelson, M.G., Khurana, K.K., Russell, C.T., Volwerk, M., Walker, R.J., Zimmer, C., 2000. Galileo magnetometer measurements: A stronger case for a subsurface ocean at Europa. Science 289, 1340–1343.

McKinnon, W.B., 1999. Convective instability in Europa's floating ice shell. Geophys. Res. Lett. 26, 951–954.

Murphy, D.M., Koop, T., 2005. Review of the vapour pressures of ice and supercooled water for atmospheric applications. Q. J. R. Meteorol. Soc. 131, 1539–1565.

Pappalardo, R.T., Head, J.W., Greeley, R., Sullivan, R.J., Pilcher, C., Schubert, G., Moore, W.B., Carr, M.H., Moore, J.M., Belton, M.J.S., Goldsby, D.L., 1998. Geological evidence for solid-state convection in Europa's ice shell. Nature 391, 365–368.

Pappalardo, R.T., et al., 1999. Does Europa have a subsurface ocean? Evaluation of the geological evidence. J. Geophys. Res. 104, 24015–24056.

Pappalardo, R.T., Barr, A.C., 2004. The origin of domes on Europa: the role of thermally induced compositional diapirism. Geophys. Res. Lett. 31, L01701, http://dx.doi.org/10.1029/2003GL019202.

Rathbun, J.A., Rodriguez, N.J., Spencer, J.R., 2010. Galileo PPR observations of Europa: Hotspot detection limits and surface thermal properties. Icarus 210, 763–769.

Scambos, T., Fricker, H.A., Liu, C.-C., Bohlander, J., Fastook, J., Sargent, A., Massom, R., Wu, A.-M., 2009. Ice shelf disintegration by plate bending and hydro-fracture: satellite observations and model results of the 2008 Wilkins ice shelf break-ups. Earth Planet. Sci. Lett. 280, 51–60.

Schenk, P.M., Chapman, C.R., Zahnle, K., Moore, J.M., 2004. Ages and interiors: the cratering record of the Galilean satellites. In: Bagenal, F., Dowling, T.E., McKinnon, W.B. (Eds.), Jupiter: The Planet, Satellites and Magnetosphere. Cambridge University Press, Cambridge, pp. 427–456.

Schmidt, B.E., Blankenship, D.D., Patterson, G.W., Schenk, P.M., 2011. Active formation of 'chaos terrain' over shallow subsurface water on Europa. Nature 479, 502–505.

Showman, A.P., Han, L., 2005. Effects of plasticity on convection in an ice shell: Implications for Europa. Icarus 177 (2), 425–437.

Slack, G.A., 1980. Thermal conductivity of ice. Phys. Rev. B 22 (6), 3065–3071.

Spencer, J.R., Tamppari, L.K., Martin, T.Z., Travis, L.D., 1999. Temperatures on Europa from Galileo PPR: nighttime thermal anomalies. Science 284, 1514–1516.

Zahnle, K., Dones, L., Levison, H.F., 1998. Cratering rates on the Galilean satellites. Icarus 136, 202–222.